Exp Oncol 2011
33, 1, 33–41

Experimental ONCOLOGY

A NOVEL MECA3 REGION IN HUMAN 3p21.3 HARBORING PUTATIVE TUMOR SUPPRESSOR GENES AND ONCOGENES

E. Braga[1,], W. Loginov[1], D. Khodyrev[1], I. Pronina[1], T. Kazubskaya[2], O. Bogatyrova[3], V.I. Kashuba[3,4], V.N. Senchenko[4,5], G. Klein[4], M.I. Lerman[6], L.L. Kisselev[5], E.R. Zabarovsky[4,5,*]*

[1]*Russian State Genetics Center, Moscow 117545 Russia*

[2]*Blokhin Cancer Research Center, Russian Academy of Medical Sciences, Moscow 115478 Russia*

[3]*Institute of Molecular Biology and Genetics, National Academy of Sciences of Ukraine, Kiev 03143, Ukraine*

[4]*Microbiology and Tumor Biology Center, Department of Clinical Science and Education, Sodersjukhuset, Karolinska Institute, Stockholm 17177, Sweden*

[5]*Engelhardt Institute of Molecular Biology, Russian Academy of Sciences, Moscow 119991, Russia*

[6]*Cancer-Causing Genes Section, Laboratory of Immunobiology, Center for Cancer Research, National Cancer Institute-Frederick, Frederick, MD 21702, USA*

***Background*: Human chromosome arm 3p is often affected in various epithelial tumors, and several tumor suppressor genes were recently identified in this region. The most affected is 3p21 region that is 50–100% rearranged in more than 30 types of malignancies, mostly in epithelial cancers: lung, breast, ovarian, cervical, kidney, head and neck, nasopharyngeal, colon etc. These cancers are responsible for 90% of cancer deaths. *Aim*: To perform the detailed analysis of 3p (especially 3p21 region) to discover novel potential oncogenes and/or tumor suppressors. *Methods*: To find novel "hot spots" and genes involved in major cancers, dense 3p microsatellite markers (altogether 24) were allelotyped in four epithelial carcinomas (272 patients in total): breast (BC), renal cell (RCC), non-small cell lung (NSCLC) and epithelial ovarian (EOC) cancers. *Results*: As a main result, a novel region, frequently affected in BC, RCC, NSCLC and EOC was localized between markers D3S2409 and D3S3667 in the 3p21.3. This region (MECA3, major epithelial cancers affected region No. 3) covers numerous UniGene clusters, including genes involved in vital cell functions and carcinogenesis (e.g. *MST1*, *MSTR1/RON*, *GPX1* and *RHOA*). The homozygous deletions were detected in the *GPX1* in RCC (12%, 6 of 50 cases) and BC (1 of 37 cases). At the same time, amplifications and multiplications within the *RHOA* putative oncogene were identified in BC and RCC. *Conclusions*: The data suggest that genes with potential oncogenic features are located in the close proximity to putative tumor suppressor gene(s) (TSG(s)) in the MECA3. Multiplication of the *RHOA* was not reported before. Significant correlation of allelic alterations in the, AP20, MECA3 and LUCA regions with tumor progression was found for some common histological tumor subtypes (e.g. clear cell RCC, and serous EOC).**

***Key Words:* human chromosome 3p, homozygous deletion, tumor suppressor gene, gene multiplication, oncogene, tumor progression**

Carcinogenesis is a multi-step genetic process that involves mutational activation of proto-oncogenes and inactivation/silencing of tumor suppressor genes (TSGs). Identification of genes causally related to the neoplastic process is essential to elucidate signaling pathways in oncogenesis. Additionally, these genes and their products could be used to design new cancer biomarkers to improve early diagnosis, predict treatment strategies and disease course.

Epithelial cancers comprise majority of all human malignancies and are associated with a high risk of poor prognosis. The short arm of chromosome 3 (3p) is frequently involved in the origin and/or development of numerous common solid tumors [1]. Transfer of 3p subchromosomal fragments via microcell hybrids indicated that different regions of normal 3p could suppress tumorigenic phenotype of cancer cell lines. The data describing 3p alterations in lung, kidney and other epithelial cancers appeared long ago [1]. However, only recently significant progress has been achieved in identifying candidate for TSG(s) and their role in oncogenesis [2–4]. For some of these genes (e.g. *RASSF1A*, *RASSF1C, NPRL2/G21*, *RBSP3/HYA22, SEMA3B, SEMA3F, FUS1* and others) tumor suppression activity was demonstrated [3–10].

Loss of heterozygosity and allelic imbalance (AI) of polymorphic markers were frequently observed in several chromosome 3p regions in various tumors, and these observations were commonly used for localization and positional cloning of TSG(s). However, since various groups applied different subsets of 3p polymorphic markers, comparison of these data was seriously complicated [1, 3]. It seems reasonable to apply an identical marker set to compare genomic alterations of 3p in different tumors. Since 3p spans up to 100 Mb most likely some crucial sites simply remain unknown. In our previous studies we compared chromosome 3p in three cancer types: clear cell renal cell carcinoma (RCC), breast (BC) and non-small cell lung (NSCLC). Common and cancer specific "hot spot" regions were mapped in 3p using identical polymorphic markers [11, 12]. Results of 3p microsatellite analysis were consistent with Real time PCR assay data [13, 14].

Received: February 3, 2011.

*Correspondence: Fax: +46-8-31-94-70; 7-495-315-05-01;
E-mail: Eugene.Zabarovsky@ki.se;
ebraga@genetika.ru

Abbreviations used: 3p – short arm of chromosome 3; AI – allelic imbalance; AP20 – Alu PCR clone 20 region; BC – breast carcinoma; CER – common eliminated region; EOC – epithelial ovarian carcinoma; HD – homozygous deletions; LOH – loss of heterozygosity; LUCA – lung cancer candidate genes region; MECA3 – major epithelial cancers affected region No. 3; NSCLC – non-small cell lung carcinoma; RCC – renal cell carcinoma; TSG – tumor suppressor gene.

In this work identical and dense 3p markers and representative subsets of tumors (272 patients in total) were examined in four cancer types: BC, RCC, NSCLC and epithelial ovarian carcinoma (EOC). AI frequencies were compared in four/five common epithelial tumors. This allowed identifying four major affected regions: LUCA, AP20 and *RARβ2* gene regions that were defined previously [1–4], and a novel critical region of 600 kb size located in 3p21.31 between D3S2409 and D3S3667 markers. This region was named MECA3, major epithelial cancers affected region in 3p21.3 No. 3. The peak around MECA3 was proven statistically using Fisher exact test ($P < 10^{-3}$). Copy number assay of *GPX1* and *RHOA* resident genes suggested close location of putative TSG(s) and oncogene(s) within this genomic segment. Significant correlation of allelic alterations in the main critical 3p regions with tumor progression was found for common histological tumor subtypes (clear cell RCC, serous EOC, and ductal BC).

MATERIALS AND METHODS

Tissues and DNA samples. Tissues were taken from patients not treated by radio- or chemotherapy. The study was approved by Ethical Committee, and each patient gave a written consent. Tumors were classified by TNM and stage according to UICC [15]. Histological typing of tumors was performed in accordance with international protocols [16–18]. 95 BC cases included mainly ductal (65 cases) and lobular (20 cases) breast carcinomas; 80 RCC cases were represented by clear cell histology type only; 47 NSCLC were represented by squamous cell lung cancer (38 cases) and adenocarcinoma (9 cases); 50 EOC consisted of diverse histological types, including 32 cases of serous adenocarcinoma. Patients of each tumor type were divided into clinical sub-groups using TNM stages (I+II *vs.* III+IV), tumor malignancy grade (1 + 2 *vs.* 3), or level of tumor differentiation (high (H) + medium (M) *vs.* low (L)). To compare the main clinical groups (early and more advanced tumors) and to use more representative subsets, stages I, II *a*, II *b*, III, *a*, *b*, *c,* and IV were not considered separately. The same approach was used in regard to differentiation level or tumor grades.

Top and bottom sections (3–5 μm thick) cut from frozen tumor tissues were examined by staining with haematoxylin and eosin. Selected samples (containing 70% or more tumor cells) and matched normal control tissues were stored at -70 °C. DNA was isolated by overnight treatment with proteinase K at 50 °C, followed by phenol/chloroform extraction and precipitation with ethanol. DNA preparations were examined by electrophoresis in 0.8% agarose gels. DNA concentration was measured in comparison to λ-phage DNA (Fermentas, Vilnius, Lithuania).

Polymorphic microsatellite markers and analysis of allelic alterations. The order of polymorphic markers on 3p, used in this study, was based on NCBI data (Build 33) and UCSC Browser data (Fig. 1). Primers for microsatellite markers were from GenBank Amplicon databases. Location of marker NL1-024/D3S4285 and primers for this locus were determined in our previous studies [19–22]. PCR and polyacrylamide gel electrophoresis were performed as described earlier [11]. Band intensities for PCR products of high and low molecular weight alleles in tumor and matched normal DNA were compared using a Molecular Dynamics Personal Densitometer SI (Sunnyvale, CA, USA) according to the manufacturer's protocol. Loss of one allele was scored only in case when reduction of intensity of this allele was more than 50%. Amplification of the second parent allele was scored when its intensity in tumor DNA was increased two folds or more. PCR was performed using Perkin Elmer 2 (Wellesley, MA, USA) and Tercik (DNA-Technology, Moscow, Russia) cyclers.

Multiplex PCR with microsatellites and non-polymorphic gene-markers. Multiplex PCR was used to confirm amplification events, allelic losses and to analyze copy number changes of fragments within *RHOA* and *GPX1* genes in some tumor cases. Multiplex PCR with polymorphic loci was performed in conditions suitable for the three markers D3S2406, p33715 and D3S2456 used in these studies. The PCR reactions were performed in a total volume of 50 μl containing 1× Taq PCR buffer [67 mM Tris-HCl, pH 9.3, 16.7 mM $(NH_4)_2SO_4$, 0.01% Twin-20], 2.0 mM $MgCl_2$, 20 pmole of primer per reaction, 250 μM dNTPs, 2U Taq polymerase (Fermentas), and 0.1 μg DNA as follows: 95 °C, 5 min; 35 amplification cycles (94 °C, 25 s; 58 °C , 1 min; 72 °C, 40 s) and 72 °C, 5 min. PCR products were analyzed using 1.5% agarose gel.

The fragment of the exon 3 of the *RARβ2* gene was used as an internal control in the analysis of copy number changes for *RHOA*, *GPX1, RASSF1A* and *SEMA3B*. Two primer pairs were used to detect homozygous deletions within *GPX1, RASSF1A* and *SEMA3B*.

The PCR reactions were performed in a total volume of 30 μl containing appropriate 1 × Taq PCR buffer, $MgCl_2$, 20 pmole of primer per reaction, 250 μM dNTPs, 2U Taq polymerase (Fermentas), and 0.1 μg DNA. Primers and other conditions are given in Table 1.

Table 1. Markers used for gene copy number experiments using multiplex PCR

Gene marker*	Primers	T_{ann}/Mg, mM**	PCR product, bp
GPX1	ACTTTGTTGTAACTGGGTCTTG	55 °C	548
	TGTCCTGTGTCATTGTCATTT	1.5	
GPX1-int	CGGGTGCGGTGGCTCATA	60 °C	237
	TGGCGCAATCTAGGCTCACTG	1.5	
RASSF1A	GTAAAGCTGGCCTCCAGAAACACGG	65 °C	357
	GCAGCTCAATGAGCTCAGGCTCCCC	2.5***	
RASSF1A-int	GGGGTGGGGTGTGAGGAGGGGACGAA	64 °C	150
	GGGCGGCGGGAAGGAGCTGAGGAGA	1.5	
SEMA3B	TTGAGATATTGGAGTCCACGGGTG	56 °C	450
	CAGTGTTGGCCTGGAAGACCTC	1.5	
SEMA3B-int	CCTTTGCCTGCTGAGCCCCTGGAG	64 °C	242
	ACCGCCCGCCGTGCCGTAAAGT	1.5	
RHOA	GGGAAGCCGAGCACCACCAG	64.2 °C	437
	GCTCGGGCGCACTCTCCAG	3,0***	
Control, exon	AGAGTTTGATGGAGTTGGGT	62 °C	229
3 of *RARβ2*	CATTCGGTTTGGGTCAATCC	1.5	

Note: *Fragments from the 5'-region of given genes were studied if not otherwise mentioned; **Buffer contained 60 mM Tris-HCl, pH 8.5, 10 mM 2-mercaptoethanol, 25 mM KCl, 0.1% Triton X-100 if not mentioned otherwise; ***Buffer contained 67 mM Tris-HCl, pH 8.9, 16.7 mM $(NH_4)_2SO_4$, 0.01% Tween-20.

PCR amplifications of *RASSF1A* and *RHOA* were performed under the program: 95 °C, 5 min; 30 amplification cycles (94 °C, 30 s; 63 °C, 40 s; 72 °C, 35 s) and 72 °C, 5 min. For *GPX1* and *SEMA3B* the following program was used: 95 °C, 5 min; 28 amplification cycles (94 °C, 25 s; 58 °C, 30 s; 72 °C, 25 s) and 72 °C, 5 min. PCR products were analyzed using 1.5% agarose gel.

In these experiments Tercik (DNA-Technology) cycler was used. The band intensities of PCR products were analyzed with Video-system Gel Imager and Gel Imaging and Gel Analysis (DNA-Technology, Moscow, Russia) software.

Statistical calculations. Statistical analysis was usually performed using Fisher exact test. Standard deviations (SD) for average values of AI frequencies in 3p re-

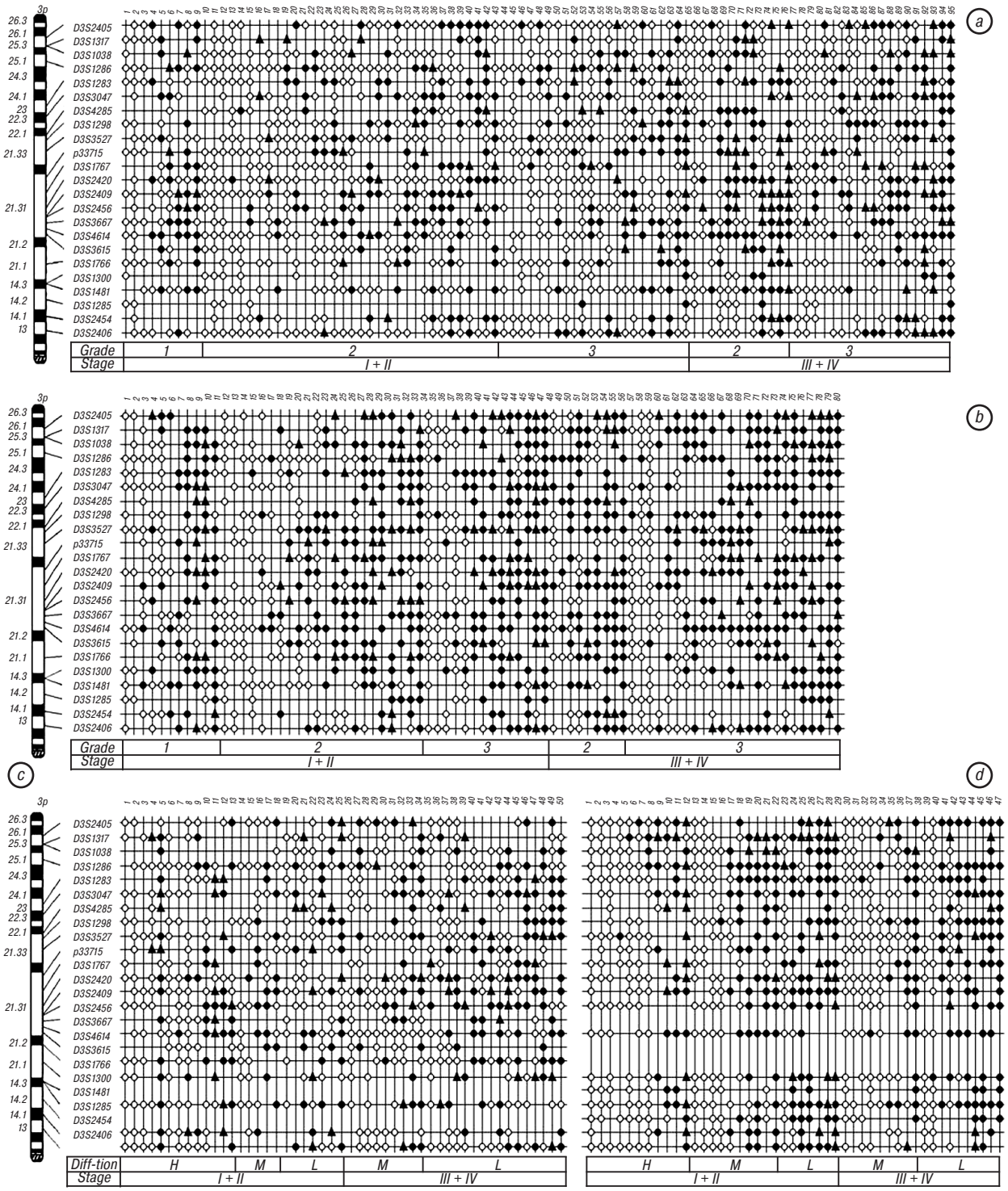

Fig. 1. Allelic alterations in 3p polymorphic markers in different tumors. (*a*) BC (95 cases); (*b*) RCC (80 cases); (*c*) EOC (50 cases); (*d*) NSCLC (47 cases). Black circles — loss of one allele; open circles — retention of both alleles; black triangles — loss of one allele with the simultaneous amplification of another allele; informative events are shown only. Diff-tion — a level of tumor differentiation in abbreviated form. H, M, and L indicate high, medium, and low level of tumor differentiation, respectively; 1, 2, 3 denote tumor malignancy grade. The main TNM stages (I, II, III, IV) were also shown. Cases with the increasing number of allelic imbalance (AI) events were localized from the left to right within the clinical variable sub-groups

gions (CI, confidential interval, 95%) were calculated as $2\{p(1\text{-}p)/2n\}^{1/2}$, where n is the number of informative events and p is the average values of AI frequencies [23].

RESULTS

Pattern of AI in 3p in five epithelial tumor types. The set of identical 3p markers were used to examine the representative subsets of RCC, BC, NSCLC and EOC samples. As shown on Fig. 2, patterns of allelic alterations were mainly represented by loss of one allele, and allelic losses accompanied by amplifications of the second allele. Allelic imbalances (AI) events in the 3p loci were summarized in Fig. 1. Percentage of tumor cases with allelic losses was high: 93% (74/80) in RCC, 88% (84/95) in BC, 84% (42/50) in EOC and 79% (37/47) in NSCLC. It is believed that terminal deletions appear from mitotic recombination [24, 25]. Interstitial deletions can indicate location of TSG(s). Terminal deletions were found rather frequent in RCC (29%) and NSCLC (34%) only. Multiple interstitial deletions were in prevalence to terminal deletions in each tumor type under the study: 64% *vs*. 29% in RCC, 45% *vs*. 34% in NSCLC, 85% *vs*. 3% in BC, 82% *vs*. 2% in EOC and 77% *vs*. 2% in CC (P << 0.05). These results indicate the existence of several putative TSG(s) in chromosome 3p.

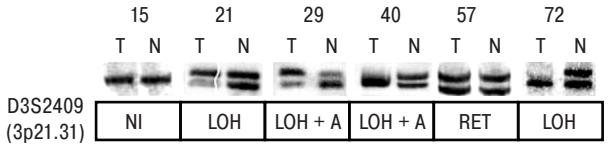

Fig. 2. Examples of various AI events, including allelic losses, loss of one allele with the simultaneous amplification of another allele, retention and non-informative cases

Chromosome 3p "hot spots" affected in major epithelial tumors. The AI frequencies were scored in four tumor types for the 3p markers to estimate the contribution of different regions of 3p to various tumor types (Table 2). To localize novel region(s) potentially harboring TSG(s) or protooncogene(s), the values of AI frequencies in the peaks were compared with the average values for the 3p markers scored for the corresponding tumor type (see Table 2, bottom). In AI pro-

Table 2. Allelic imbalance frequencies in epithelial tumors (*)

3p SUB-REGIONS**	MARKER	LOCATION***	RCC (80 cases)	NSCLC (47 cases)	BC (95 cases) ****	EOC (50 cases)
#1	D3S2405	3p25.3	37/48, 77%	19/34, 56%	31/72, 43%	10/27, 37%
	D3S1317	3p25.3	35/49, 71%	19/33, 58%	22/63, 35%	8/21, 38%
	D3S1038	3p25.3	35/50, 70%	13/30, 43%	15/44, 34%	8/21, 38%
#2	D3S1286	3p25.1	30/55, 55%	23/42, 55%	26/71, 37%	14/42, 33%
#3	D3S1283	3p23	34/49, 69%	19/37, 51%	29/60, 48%	13/27, 48%
	D3S3047	3p22.3	33/44, 75%	18/33, 55%	32/60, 53%	17/36, 47%
#4	D3S4285	3p21.33	22/27, 81%,	9/18, 50%	19/41, 46%	10/18, 55%
(AP20)	D3S1298	3p21.33	32/48, 67%	17/31, 55%	29/58, 50%	11/26, 42%
#5	D3S3527	3p21.33	43/59, 73%	14/33, 42%	24/71, 34%	15/37, 41%
	P33715	3p21.31	20/33, 61%	9/25, 36%	26/52, 50%	12/24, 50%
	D3S1767	3p21.31	33/49, 67%	14/27, 52%	25/52, 48%	9/21, 43%
	D3S2420	3p21.31	35/45, 78%	16/35, 46%	27/68, 40%	18/37, 49%
#6	D3S2409	3p21.31	29/42, 69%	19/32, 59%	39/69, 57%§	18/37, 49%
(MECA3)	D3S2456	3p21.31	35/45, 78%	12/28, 43%	33/59, 56%§§	17/37, 46%
	D3S3667	3p21.31	30/45, 67%	No data	34/59, 58%§§§	11/22, 50%
#7 (LUCA)	D3S4614	3p21.31	41/60, 68%	17/34, 50%	36/75, 48%,	17/41, 41%
#8	D3S3615	3p21.2	30/48, 63%	No data	15/37, 41%	8/21, 38%
	D3S1578	3p21.2	No data	No data	No data	14/34, 41%,
	D3S1766	3p21.1	31/49, 63%	15/32, 47%	20/54, 37%	12/25, 48%
	D3S1300	3p14.3	24/33, 73%	7/18, 39%	6/20, 30%	No data
	D3S1481	3p14.3	29/55, 53%	21/42, 50%	22/68, 32%	14/38, 37%
#9	D3S1285	3p14.2	13/24, 54%	10/25, 40%	4/15, 27%	No data
	D3S2454	3p14.1	17/35, 49%	11/21, 52%	19/48, 40%	11/28, 39%
	D3S2406	3p13	33/60, 55%	12/33, 36%	25/75, 33%	13/37, 35%
	Average values	3p25.3-3p13	703/1052, 67 ± 2%#	314/643, 49 ± 3%#	558/1290, 43 ± 2%#	280/657, 43 ± 3%#

Note: *AIs divided by informative events number; SD (CI=95%) for the AI average values were scored as $2\{p(1\text{-}p)/2n\}^{1/2}$; AI frequencies higher than the average values were shown grey; **Twenty three markers were grouped in nine regions of 3p; ***Markers location was from NCBI (http://www.ncbi.nlm.nih.gov/cgi-bin/Entrez/map_search), Build 33; ****Significant differences between AI frequencies and average values were found for D3S2409, D3S2456 and D3S3667 markers in BC, using Fisher exact test: §P= 0,0206; §§P = 0,0373;§§§P = 0,0199.

Table 3. Average frequencies of AI events in nine 3p regions in four cancer types

Regions	#1 3p25.3 *VHL*-region	#2 3p25.12-region	#3 3p23-p22.4 *RARβ2*-region	#4 3p21.33 AP20-region	#5 3p21.33-p21.31 CER-region	#6 3p21.31 MECA3-region	#7 3p21.31 LUCA-region	#8 3p21.2-p14.3 FHIT-region	#9 3p14.2-p13 DUTT1-region
RCC	**107/147**	30/55	**67/93**	**54/75**	**131/186**	**94/132**	**41/60**	114/185	63/119
	73%	55%	**72%**	**72%**	**70%**	**71%**	**68%**	62%	53%
NSCLC	**51/97**	**23/42**	**37/70**	**26/49**	53/120	**31/60**	**17/34**	43/92	33/79
	53%	**55%**	**53%**	**53%**	44%	**52%**	**50%**	47%	47%
BC	68/179	26/71	**61/120**	**48/99**	102/243	**106/187**	**36/75**	63/179	24/65
	38%	37%	**51%**	**48%**	42%	**57%**	**48%**	35%	37%
EOC	26/69	14/42	**30/63**	**21/44**	**54/119**	**46/96**	17/41	34/84	24/65
	38%	33%	**48%**	**48%**	**45%**	**48%**	41%	40%	37%

Note: The highest average frequencies of AI events for each cancer type in specified regions are shown bold. The average values of AI frequencies in some regions were fairly higher (e.g. 5–14% in BC) in comparison with the average value of AI for all 3p markers for a given tumor and exceeded the SD (CI = 95%) for 3p markers in total (43%, Table 2, bottom). The peak in BC in region #6 (MECA3, D3S2409-D3S3667 interval) was additionally proved, using Fisher exact test with $P = 0.8\times10^{-3}$ (106/187, 57% *vs.* 558/1290, 43%, see Table 2, bottom).

files of 3p several peaks were found in each cancer. Three neighboring markers, D3S2409, D3S2456, and D3S3667, located within 3p21.31 band, displayed peaks with significant statistics for the representative subset of BC patients (P = 0.02–0.04, see Table 2). Significant differences between AI frequencies and average values were found for D3S2409, D3S2456 and D3S3667 markers in BC, using Fisher exact test: P = 0,0206; P = 0,0373; P = 0,0199.

The studied markers were divided into nine groups, and the average AI frequencies were scored for various regions in each tumor type (see Table 2, 3). This approach allowed comparing contribution of different regions along 3p in various tumors. Four regions, namely #3, 4, 6 and 7 showed the highest frequencies of AI in all five tumor types. The average values of AI frequencies in these regions were fairly higher in comparison with the average value of AI in 3p for all markers for a given tumor and exceeded the SD, CI 95% (see Table 2, 3).

Three regions are located in 3p21.3. Two of them, #4 or AP20 (marked by NL1-024/D3S4285 and D3S1298) and #7 or LUCA (marked by D3S4614) were described earlier [2, 26, 27]. The third frequently affected region in 3p21.3 (#6, marked by D3S2409, D3S2456, and D3S3667), was localized for the first time, and importance of this novel site was proven using Fisher exact test ($P < 10^{-3}$; Table 3). According to the UCSC Browser data, this D3S2409-D3S3667 region (MECA3, major epithelial cancers affected region No. 3) covers numerous UniGene clusters (~30 genes/600 kb) including genes involved in vital cell functions and carcinogenesis, e.g. *MST1*, *MSTR1/RON*, *GPX1* and *RHOA*. The contribution of these genes in processes such as apoptosis, adhesion, signal transduction, angiogenesis and others [28–33] was previously reported. MECA3 covers region of 600 kb size (49.3–49.9 Mb according to the NCBI and UCSC databases), belongs to 3p21.31 close to the LUCA region that harbors a cluster of putative and authentic TSG(s) [2–9].

Therefore, the regions #3, 4, 6 and 7 (see Table 2, 3) were frequently affected in all tested major cancers. The other regions #1, 5 and 9 (see Table 2, 3) were also found involved in some tumors. Region surrounding VHL gene (#1, see Table 2, 3) showed AI frequently in RCC and NSCLC. Common eliminated region (CER or #5, see Table 2, 3) located previously by functional assay [34], was significantly affected in RCC and EOC.

Homozygous deletions in GPX1. HDs are excellent indicators for identification of TSGs. Detection of HDs was used to discover and confirm AP20 and LUCA TSG regions in 3p.21.3 [2, 13, 14]. We screened 50 RCC and 37 BC cases for HDs within the *GPX1* using multiplex PCR with two pairs of primers for this gene and primers for the exon 3 of the *RARβ2* as an internal control (see Table 1). Copy numbers of this *RARβ2* fragment did not change in RCC and BC cases analyzed (Fig. 3, *a*). HDs were detected within *GPX1* gene rather frequently in RCC (12%, 6/50), and more rarely in BC (3%, 1/37) (see Fig. 3, *a*). For comparison, *RASSF1A* and *SEMA3B* from the LUCA region [2–4] were also tested (see Fig. 3, *b* and Table 1; data not shown). HDs in *GPX1*, *RASSF1A* and *SEMA3B* were detected with similar frequencies. HD incidence was apparently tumor and gene specific (see Fig. 3, *b*). These observations confirmed the MECA3 as a novel 3p21.3 region, potentially harboring TSG(s).

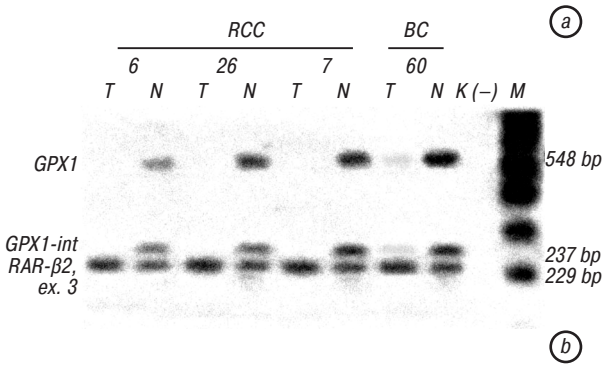

Gene	Location	RCC	BC
GPX1	MECA3	6/50, 12%	1/37, 3%
RASSF1A	LUCA	0/53, 0%	5/46, 11%
SEMA3B	LUCA	4/53, 8%	2/46, 4%

Fig. 3. Homozygous deletions in *GPX1* gene resided in the MECA3. (*a*) Representative examples of HDs, detected in *GPX1* in RCC and BC cases by multiplex PCR. Fragment of 5'-promoter region of *GPX1* was analyzed with two primer pairs and fragment of *RARβ2* (exon 3) was used as internal control. Primers, PCR conditions and programs are shown in Table 1; 1.5% agarose gel electrophoresis was used (see also Materials and Methods part). (*b*) Comparison of HDs incidence in *GPX1*, and *RASSF1A* and *SEMA3B* (TSGs in the LUCA region) in RCC and BC

Amplification events accompanying allelic losses in 3p markers. As it was mentioned above, sometimes allelic losses were found associated with amplifications of a second parent allele. Amplification events (see Fig. 1, 2) were detected in 13% (141 amplification events of 1052 informative events) of RCC, 10% (130/1290) of BC, 8% (52/643) of NSCLC, and in 9% (60/657) of EOC.

Amplification events can activate protooncogene(s) located closely to inactivated TSG(s). The non-random distribution of amplification events along 3p was observed in various cancers. The enhanced amplification frequencies within the MECA3 were proved in BC (Fig. 2, *a*). Amplification events in the MECA3 constituted 16.5% (31/187, for three markers D3S2409, D3S2456 and D3S3667; Fig. 1, *a*), that significantly higher than the average value (10%, 130/1290) for all 3p markers analyzed ($P = 0.03$). We suggested that 3p and especially the MECA3 region include putative oncogene(s) possibly located closely to TSG(s).

Amplification of RHOA/ARHA in RCC and BC. Multiplication of a particular protooncogene in tumors can be one of the reasons leading to its activation. Multiplex PCR was applied in this study to measure copy number changes of the *RHOA* in RCC and BC cases. *RHOA* covers D3S2409 and is adjacent to the D3S2456. Allelic amplifications were revealed for these markers in experiments described above (see primers in Table 1). Tumor cases showing amplifications with these markers were tested to con-

firm *RHOA* multiplication. Exon 3 of the *RARβ2* gene was used as internal control. *RHOA* gene revealed clear copy number multiplications (data not shown). Altogether we found *RHOA* multiplication /amplification varying in range 2–50 times in 12 of 17 RCC and in 14 of 19 BC cases. The finding confirmed an amplification in the MECA3 region in BC and RCC and supported putative oncogenic features of the *RHOA* gene.

Contribution of 3p allelic alterations into cancer progression. To examine contribution of 3p allelic alterations into cancer progression the most common histological subtypes like clear cell RCC, ductal and lobular BC, serous ovarian adenocarcinoma (serous EOC) and squamous cell lung cancer were analyzed. The number of affected tumor samples in a given region was divided by the total number of tumor samples and compared between groups with various clinical stage and grade or differentiation (Table 4). In summary, allelic alterations in three most important 3p21.3 regions (AP20, LUCA, and MECA3) significantly correlated with tumor progression of specific histological subtypes.

Correlations were estimated to be stronly significant for AP20 and LUCA regions in clear cell RCC (Table 4, *a*), serous EOC (Table 4, *b*), and ductal BC (not shown), and also for AP20 — in squamous cell NSCLC (not shown). The MECA3 was significantly associated with advanced clinical stages and low differentiation of serous EOC (see Table 4, *b*).

Table 4. Correlation of allelic alterations with tumor progression in clear cell RCC (A) and serous ovarian adenocarcinoma (B), revealed in 3p regions

a, Clear cell RCC

	#4 (AP20)	#7 (LUCA)
Grade	**P = 0.0421**	*P = 0.2734*
1+2	**48%, 20/42**	45%, 19/42
3	**71%, 27/38**	58%, 22/38
Stage	**P = 0.0117**	**P = 0.0248**
I+II	**47%, 22/47**	**40%, 19/47**
III+IV	**76%, 25/33**	**67%, 22/33**

b, Serous ovarian adenocarcinoma

	#4 (AP20)	#6 (MECA3)	#7 (LUCA)
Differentiation	**P = 0.0078**	**P = 0.006**	**P = 0.0496**
H+M	**8%, 1/12**	**33%, 4/12**	**8%, 1/12**
L	**60%, 12/20**	**85%, 17/20**	**45%, 9/20**
Stage	*P = 0.4501*	**P = 0.0018**	*P = 0.2593*
I+II	27%, 3/11	**27%, 3/11**	18%, 2/11
III+IV	48%, 10/21	**86%, 18/21**	38%, 8/21

Note: The percentage of tumor samples with AI in a given region relative to the total tumor samples is shown for early and advanced clinical and histological groups. Statistically significant values are shown bold.

DISCUSSION

Multiple interstitial deletions in 3p and location of several TSG(s). In this study we used an additional tumor type (EOC) and novel patients compared to our previous study [12] that was highly helpful to reduce misinterpretation of the mapping data. Fraction of terminal deletions became reduced, e.g. in RCC 29% *vs.* 50%. Discontinuous deletions were also reported earlier in previous studies [1, 12–14, 35–38]. Here prevalence of multiple interstitial deletions over terminal deletions was highly significant ($P < 0.05$) in all four analyzed tumor types. Frequent interstitial deletions were suggested to indicate a location of several cancer related genes in chromosome 3p [1, 3]. This hypothesis was recently confirmed by discovery of two clusters of putative and authentic TSG(s) in LUCA and AP20 sites [2–4, 7–10].

Novel 3p21.3 MECA3 region contains cancer related genes including putative TSG(s). Densely distributed polymorphic markers gave us the basis to compare 3p alterations in four cancer types and to define four regions the most frequently affected in major epithelial tumors. The use of 13 markers for the 3p21 band, which was previously shown to be the most significant for malignant transformation [1, 3], allowed us to delineate at least three important regions inside this band. One of these regions, MECA3 between D3S2409 and D3S3667 was identified here for the first time. The position of the MECA3 was consistent with the highest LOH frequency in 3p21.3, reported for BC earlier [38]. Our studies provided first statistically significant evidence for the AI peak in MECA3 ($P < 0.001$). The results suggested that the MECA3 could harbor TSG(s). According to the UCSC Browser data, numerous UniGenes clusters are located in the MECA3 including genes (e.g. *RHOA/ARHA, GPX1, MST1, MSTR1/RON, USP4* and *DAG1*) involved in vital cell functions (such as apoptosis, adhesion, signal transduction, angiogenesis and others) related to malignant transformation or tumor progression [28–33].

Antioxidant selenoprotein GPX1 metabolizing H_2O_2 to O_2 and H_2O represents the most commonly expressed member of the glutation peroxidase gene family. The protein is localized in mitochondria, nucleus and cytosol [39]. Decreased expression of *GPX1* was reported in various tumors [29, 40, 41]. *GPX1* plays a central role in protection of cells against oxidative damage [29, 39]. Down-deregulated expression can indirectly point to tumor suppressive features. Indeed, *GPX1* over-expression was found to delay growth of the endothelial cell line, ECV304 [42]. Relation of *GPX1* activity with malignancy is also based on p53 inducible activation of *GPX1* transcription through the interaction of its promoter region with p53 as a transcription factor [43]. One of the reasons leading to the loss of expression could be a homozygous deletion of a whole or part of the gene. *GPX1* was tested here for HDs in RCC and BC in comparison with *RASSF1A* and *SEMA3B*. Using multiplex PCR, HDs were detected in *GPX1* gene in these tumors with frequencies of up to 12%, and in *RASSF1A* and *SEMA3B* with frequencies of up to 11% and 8%, respectively. More sensitive quantitative Real Time PCR revealed 10–18% of HDs in RCC and BC within the NL3-001 marker closely located to *SEMA3B* in our previous study [14]. Nevertheless, incidence of HDs in tumors was similar for these three genes. These data support TSG features of *GPX1* and suggested that the MECA3 potentially harbor TSG(s).

The chromosomal regions around *VHL* (3p25.3), CER (3p21.31), and proximal region in 3p14.2-p13 were shown to be a tumor-specific. Region around VHL gene

showed AI mainly in RCC and NSCLC. CER was affected mainly in RCC and EOC.

Both putative oncogenes and TSG(s) could be located in the MECA3. AI pattern was complex in many tumor biopsies and amplification of a second allele was frequently (up to 13% in RCC cases) observed in addition to LOH. LOH associated with amplification in 3p was detected earlier in lung cancer by combination of allelotyping with FISH [44]. We showed that distribution of amplification events was not random along 3p, including an amplification peak within the MECA3 region in BC with significant statistics (P = 0.03). These data suggested that the MECA3 contains both TSG(s) and oncogene(s).

Amplification is one of the possible mechanisms of proto-oncogene activation. In this work we studied amplification of the *RHOA* also known as *ARHA* gene. Rho small GTPases are members of the Ras-superfamily. *RHOA* gene was reported to be involved in critical cellular functions such as cell growth, development, apoptosis, and cell cyto-architecture (the formation of stress fibers, and focal adhesions). The gene is also important for cell-cell dissociation and motility. *RHOA* is deregulated during tumor progression and it is suggested that the pivotal steps in this process are adhesion of tumor cells to the host cell layers and subsequent migration in cancer invasion and metastasis [28, 45]. Activation of *RHOA*, regulating the microfilament network and cadherin-dependent cell-cell contacts, leads to the induction of cellular proliferation, morphological transformation, anchorage-independent growth, and tumor formation when transformed cells are injected into nude mice. Recent evidence has suggested that *RHOA* could also act as a dominant oncogene, since *RHOA* transgenes confer a transformed phenotype on fibroblast cells in culture. *RHOA* exhibited an elevated expression on protein and RNA level in BC, EOC and testicular tumors [28, 46, 47]. Activating mutations were not detected in the coding region of this putative oncogene neither in BC, RCC, lung, colon or ovarian carcinomas [48]. Over-expression of a gene in certain tumor types could be causally associated with the elevated gene copy numbers. Here multiplication of the *RHOA* genomic copies in some BC and RCC was reported for the first time. The amplification of the *RHOA* gene was shown to be associated with the increased expression on RNA level in BC, RCC and EOC by us earlier. The degree of multiplication/amplification observed directly in *RHOA* gene achieved 2-50 fold in RCC and BC. The incidence of amplification events within MECA3 in BC achieved 16.5%.

Multiplications and amplifications of the *RHOA* in BC and RCC supported its oncogenic behavior and can represent a model of the *RHOA* activation never reported before for this putative oncogene. These experiments also confirmed the hypothesis that TSG(s) and oncogene(s) can be closely located and even the same gene (*RHOA*) can sometimes play TSG or oncogenic role [see also 10 and 49].

3p genes contribute to tumor progression. In this study four regions of 3p were affected in the major cancer types and were found to be associated with progression of certain histological types of tumors. Earlier association with tumor progression was revealed mainly for proximal and telomeric regions of 3p. Thus, AI in 3p24-p25 markers in BC was found to correlate with histological grade [50] and risks of five years mortality [51]. Increased frequency of allelic losses of 3p markers in BC was also associated with increasing tumor grade [52]. High frequency of LOH events in 3p25 and 3p14 markers was shown to correlate with the stage of EOC [53]. Allelic losses at 3p14 and in the telomeric region of 3p21.3 were reported to accumulate predominantly in low differentiated lung adenocarcinoma [54].

Here, a systematic study was performed in detail using identical set of markers distributed along 3p in representative subsets of major epithelial tumors, characterized histologically and clinically. In search for a possible association of 3p alteration with tumor progression, the most common histological subtypes were considered: clear cell RCC, ductal and lobular BC, serous EOC and squamous cell lung cancer. The nine 3p regions were tested, and allelic alterations in four regions, especially the AP20, LUCA, and MECA3, were shown to be significantly associated with progression of several histological types of tumors. Contribution of AP20 and LUCA regions to the progression of clear cell RCC, and serous EOC, and association of the allelic changes in the MECA3 with advanced stages and poor differentiation of serous EOC was proved using calculation approach based on tumor samples numbers and AI events numbers (Table 4).

Thus, we provided evidence of relationship between progression of several histological tumor types and allelic alterations within the regions in the 3p21.3 band. Our findings suggest that some genes located in these 3p21.3 segments are involved in the progression of certain epithelial cancers in addition to the well-documented role of 3p genes in the early events of neoplasm development [1, 3].

CONCLUSION

As a main result, a novel region frequently affected in four major epithelial cancers was localized between markers D3S2409 and D3S3667 in the 3p21.3. This region (MECA3, major epithelial cancers affected region No. 3) covers numerous UniGene clusters, including genes involved in vital cell functions and carcinogenesis (e.g. *MST1*, *MSTR1/RON*, *GPX1* and *RHOA*). The homozygous deletions were detected in the *GPX1* in RCC (12%, 6 of 50 cases) and BC (1 of 37 cases). The data suggested that genes with oncogenic features are located in the close proximity to putative TSG(s) in the MECA3. *RHOA* multiplication, never reported before, can represent a novel mode of this protooncogene activation. Significant correlation of allelic alterations in the AP20, MECA3 and LUCA regions with tumor progression was found for some

common histological tumor subtypes (clear cell RCC, serous EOC, and ductal BC).

ACKNOWLEDGEMENTS

This work was supported by grants 08-04-01577 and 10-04-01213 from the Russian Foundation for Basic Research; State Contracts 02.740.11.5227 and 16.740.11.0173 with the Russian Ministry of Education and Science. VIK and OB was supported by the National Academy of Sciences of Ukraine. ERZ was supported by grants from the Swedish Cancer Society, the Swedish Research Council, the Swedish Institute and Karolinska Institute.

REFERENCES

1. **Kok K, Naylor SL, Buys CHCM.** Deletions of the short arm of chromosome 3 in solid tumors and the search for suppressor genes. Adv Cancer Res 1997; **71**: 27–92.

2. **Lerman MI, Minna JD.** The 630-kb lung cancer homozygous deletion region on human chromosome 3p21.3: identification and evaluation of the resident candidate tumor suppressor genes. The International Lung Cancer Chromosome 3p21.3 Tumor Suppressor Gene Consortium. Cancer Res 2000; **60**: 6116–33.

3. **Zabarovsky ER, Lerman MI, Minna JD.** Tumor suppressor genes on chromosome 3p involved in the pathogenesis of lung and other cancers. Oncogene 2002; **21**: 6915–35.

4. **Imreh S, Klein G, Zabarovsky E.** Search for unknown tumor antagonizing genes. Genes Chrom Cancer 2003; **38**: 307–21.

5. **Dammann R, Schagdarsurengin U, Strunnikova M, *et al.*** Epigenetic inactivation of the Ras-association domain family 1 (*RASSF1A*) gene and its function in human carcinogenesis. Histol Histopathol 2003; **18**: 665–77.

6. **Vos MD, Martinez A, Elam C, *et al.*** A role for *RASSF1A* tumor suppressor in the regulation of tubulin polymerization and genomic stability. Cancer Res 2004; **64**: 4244–50.

7. **Dreijerink K, Braga E, Kuzmin I, *et al.*** The candidate tumor suppressor gene, *RASSF1A*, from human chromosome 3p21.3 is involved in kidney tumorigenesis. Proc Natl Acad Sci USA 2001; **98**: 7504–9.

8. **Li J, Wang F, Protopopov A, *et al.*** Inactivation of *RASSF1C* during in vivo tumor growth identifies it as a tumor suppressor gene. Oncogene 2004; **23**: 5941–9.

9. **Li J, Wang F, Haraldson K, *et al.*** Functional characterization of the candidate tumor suppressor gene *NPRL2/G21* located in 3p21.3C. Cancer Res 2004; **64**: 6438–43.

10. **Kashuba VI, Li J, Wang F, *et al.*** *RBSP3* (*HYA22*) is a tumor suppressor gene implicated in major epithelial malignancies. Proc Natl Acad Sci USA 2004; **101**: 4906–11.

11. **Braga E, Pugacheva E, Bazov I, *et al.*** Comparative allelotyping of the short arm of human chromosome 3 in epithelial tumors of four different types. FEBS Lett 1999; **454**: 215–9.

12. **Braga E, Senchenko V, Bazov I, *et al.*** Critical tumor-suppressor gene regions on chromosome 3p regions in major human epithelial malignancies: allelotyping and quantitative real time PCR. Int J Cancer 2002; **100**: 534–41.

13. **Senchenko V, Liu J, Braga E, *et al.*** Deletion mapping of cervical carcinomas using quantitative real-time PCR identifies two frequently affected regions in 3p21.3. Oncogene 2003; **22**: 2984–92.

14. **Senchenko V, Liu J, Loginov W, *et al.*** Discovery of frequent homozygous deletions in chromosome 3p21.3 LUCA and AP20 regions in renal, lung and breast carcinomas. Oncogene 2004; **23**: 5719–28.

15. **Sobin LY, Wittekind Ch, *eds.*** UICC TNM classification of malignant tumors. 6th ed. New York: Wiley-Liss Inc., 2002. 264 p.

16. **Tavassoli FA, Devilee P, *eds*.** World Health Organization: Classification of tumors. Pathology and genetics of tumors of the breast and female genital organs. Lyon: IARCPress, 2003. 432 p.

17. **Eble JN, Sauter GS, Epsten JI, *et al, eds*.** World Health Organization: Classification of tumors. Pathology and genetics. Tumors of the urinary system and male genital organs. Lyon: IARCPress, 2004. 360 p.

18. **Travis WD, Colby TV, Corrin B, *et al, eds*.** Histological typing of lung and pleural tumors. 3rd ed. Berlin-Heidelberg: Springer-Verlag, 1999. 156 p.

19. **Braga EA, Kotova EJ, Pugacheva EM, *et al.*** Human chromosome 3: detection of microsatellites of di-, tri-, and tetra-motifs, analysis of its allocation and markers formation. Mol Biol (Moscow) 1997; **31**: 985–96.

20. **Kashuba VI, Gizatullin RZ, Protopopov AI, *et al.*** Analysis of NotI linking clones isolated from human chromosome 3 specific libraries. Gene 1999; **239**: 259–71.

21. **Sulimova GE, Kutsenko AS, Rakhmanaliev ER, *et al.*** Human chromosome 3: integration of 60 NotI clones into a physical and gene map. Cytogenet Genome Res 2002; **98**: 177–83.

22. **Sulimova GE, Rakhmanaliev ER, Klimov EA, *et al.*** NotI-STS markers for human chromosome 3 are gene markers. Mol Biol (Moscow) 2005; **39**: 593–607.

23. **Weir BS.** Genetic data analysis. Methods for Discrete Population Genetic Data. Sunderland, MA: Sinauer, 1990. 377 p.

24. **De Nooij-vanDalen AG, van Buuren-van Seggelen VHA, Lohman PHM, *et al.*** Chromosome loss with concomitant duplication and recombination both contribute most to loss of heterozygosity in vitro. Genes Chrom Cancer 1998; **21**: 30–8.

25. **Thiagalingam S, Laken S, Willson JKV, *et al.*** Mechanisms underlying losses of heterozygosity in human colorectal cancers. Proc Natl Acad Sci USA 2001; **98**: 2698–702.

26. **Rimessi P, Gualandi F, Morelli C, *et al.*** Transfer of human chromosome 3 to an ovarian carcinoma cell line identifies three regions on 3p involved in ovarian cancer. Oncogene 1994; **9**: 3467–74.

27. **Protopopov A, Kashuba V, Zabarovska VI, *et al.*** An integrated physical and gene map of the 3.5-Mb chromosome 3p21.3 (AP20) region implicated in major human epithelial malignancies. Cancer Res 2003; **63**: 404–12.

28. **Pille JY, Denoyelle C, Varet J, *et al.*** Anti-RhoA and anti-RhoC siRNAs inhibit the proliferation and invasiveness of MDA-MB-231 breast cancer cells *in vitro* and *in vivo*. Mol Ther 2005; **11**: 267–74.

29. **Hu YJ, Diamond AM.** Role of glutathione peroxidase 1 in breast cancer: loss of heterozygosity and allelic differences in the response to selenium. Cancer Res 2003; **63**: 3347–51.

30. **Lee KK, Ohyama T, Yajima N, *et al.*** MST, a physiological caspase substrate, highly sensitizes apoptosis both upstream and downstream of caspase activation. J Biol Chem 2001; **276**: 19276–85.

31. **Peace BE, Hughes MJ, Degen SJF, *et al.*** Point mutations and overexpression of Ron induce transformation, tumor formation, and metastasis. Oncogene 2001; **20**: 6142–51.

32. **DeSalle LM, Latres E, Lin D, *et al.*** The de-ubiquitinating enzyme Unp interacts with the retinoblastoma protein. Oncogene 2001; **20**: 5538–42.

33. **Sgambato A, Migaldi M, Montanari M, *et al.*** Dystroglycan expression is frequently reduced in human breast and

colon cancers and is associated with tumor progression. Am J Pathol 2003; **162**: 849–60.

34. **Kholodnyuk I, Kost-Alimova M, Yang Y, *et al.*** The microcell hybrid-based "elimination test" identifies a 1-Mb putative tumor-suppressor region at 3p22.2-p22.1 centromeric to the homozygous deletion region detected in lung cancer. Genes Chrom Cancer 2002; **34**: 341–4.

35. **Fullwood P, Marchini S, Rader JS, *et al.*** Detailed genetic and physical mapping of tumor suppressor loci on chromosome 3p in ovarian cancer. Cancer Res 1999; **59**: 4662–7.

36. **Alimov A, Kost-Alimova M, Liu J, *et al.*** Combined LOH/CGH analysis proves the existence of interstitial 3p deletions in renal cell carcinoma. Oncogene 2000; **19**: 1392–9.

37. **Wistuba II, Behrens C, Virmani AK, *et al.*** High resolution chromosome 3p allelotyping of human lung cancer and preneoplastic/preinvasive bronchial epithelium reveals multiple, discontinuous sites of 3p allele loss and three regions of frequent breakpoints. Cancer Res 2000; **60**: 1949–60.

38. **Maitra A, Wistuba II, Wachington C, *et al.*** High-resolution chromosome 3p allelotyping of breast carcinomas and precursor lesions demonstrates frequent loss of heterozygosity and a discontinuous pattern of allele loss. Am J Pathol 2001; **159**: 119–30.

39. **Diwadkar-Navsariwala V, Diamond AM.** The link between selenium and chemoprevention: a case for selenoproteins. J Nutr 2004; **134**: 2899–902.

40. **Korotkina RN, Matskevich GN, Devlikanova ASh, *et al.*** Activity of glutathione-metabolizing and antioxidant enzymes in malignant and benign tumors of human lungs. Bull Exp Biol Med 2002; **133**: 606–8.

41. **Hasegawa Y, Takano T, Miyauchi A, *et al.*** Decreased expression of glutathione peroxidase mRNA in thyroid anaplastic carcinoma. Cancer Lett 2002; **182**: 69–74.

42. **Faucher K, Rabinovitch-Chable H, Barriere G, *et al.*** Overexpression of cytosolic glutathione peroxidase (GPX1) delays endothelial cell growth and increases resistance to toxic challenges. Biochimie 2003; **85**: 611–7.

43. **Tan M, Li S, Swaroop M, *et al.*** Transcriptional activation of the human glutathione peroxidase promoter by p53. J Biol Chem 1999; **274**: 12061–6.

44. **Varella-Garcia M, Gemmill RM, Rabenhorst SH, *et al.*** Chromosomal duplication accompanies allelic loss in non-small cell lung carcinoma. Cancer Res 1998; **58**: 4701–7.

45. **Zhou H, Kramer RH.** Integrin engagement differentially modulates epithelial cell motility by RhoA/ROCK and PAK1. J Biol Chem 2005; **280**: 10624–35.

46. **Horiuchi A, Imai T, Wang C, *et al.*** Up-regulation of small GTPases, RhoA and RhoC, is associated with tumor progression in ovarian carcinoma. Lab Invest 2003; **83**: 861–70.

47. **Kamai T, Yamanishi T, Shirataki H, *et al.*** Overexpression of RhoA, Rac1, and Cdc42 GTPases is associated with progression in testicular cancer. Clin Cancer Res 2004; **10**: 4799–805.

48. **Moscow JA, He R, Gnarra JR, *et al.*** Examination of human tumors for *rhoA* mutations. Oncogene 1994; **9**: 189–94.

49. **Senchenko VN, Krasnov GS, Dmitriev AA, *et al.*** Differential Expression of the CHL1 Gene during Development of Major Human Cancers. PLoS ONE, in press.

50. **Yang Q, Yoshimura G, Sakurai T, *et al.*** Allelic loss of chromosome 3p24 correlates with tumor progression rather than with retinoic acid receptor β2 expression in breast carcinoma. Breast Cancer Res and Treat 2001; **70**: 39–45.

51. **Matsumoto S, Minobe K, Utada Y, *et al.*** Loss of heterozygosity at 3p24-p25 as a prognostic factor in breast cancer. Cancer Lett 2000; **152**: 63–9.

52. **Martinez A, Walker RA, Shaw JA, *et al.*** Chromosome 3p allele loss in early invasive breast cancer: detailed mapping and association with clinicopathological features. Mol Pathol 2001; **54**: 300–6.

53. **Zhang G-L, Xu K-L.** Loss of heterozygosity at chromosome 3p in epithelial ovarian cancer in China. Int J Gynecol Cancer 2002; **12**: 198–201.

54. **Iijima H, Tomizawa Y, Dobashi K, *et al.*** Allelic losses on chromosome 3p are accumulated in relation to morphological changes of lung adenocarcinoma. Br J Cancer 2004; **91**: 1143–8.